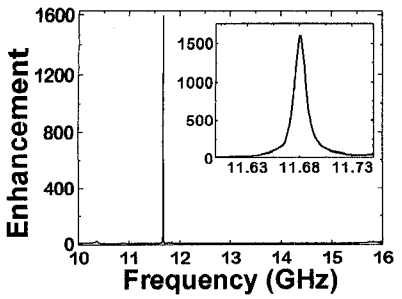


**QTuJ2 Fig. 2.** The measured power of the EM field inside a one-dimensional defect structure.

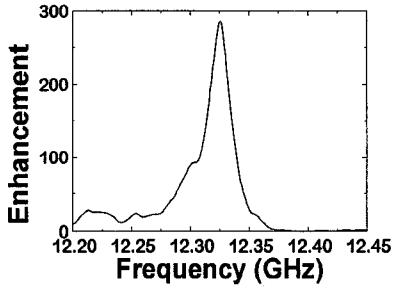


**QTuJ2 Fig. 3.** The measured power of the EM field inside a localized defect structure.

crystal structure in the following manner. Part of the rods on the 8th and 9th layers were removed to obtain a rectangular prism like cavity. Figure 3 shows the power enhancement characteristics of this structure. An enhancement factor of 290, and a *Q*-factor of 540 were measured at a defect frequency of 12.32 GHz.

Our results suggest the possibility of using the embedded detector as an RCE detector. By using a smaller size photonic crystal and a higher-frequency detector, the effect can also be shown at millimeter and far-infrared frequencies. Such RCE detectors will have increased sensitivity and efficiency when compared to conventional detectors, and can be used for various applications where sensitivity and efficiency are important parameters.

**Ames Laboratory and Microelectronics Research Center, Iowa State University, Ames, Iowa 50011*

1. E. Yablonovitch *et al.*, Phys. Rev. Lett. **63,** 1950 (1989).
2. K.M. Ho *et al.*, Solid State Comm. **89,** 413 (1994).
3. E. Ozbay *et al.*, Phys. Rev. B **51,** 13961 (1995).
4. E. Ozbay *et al.*, Appl. Phys. Lett. **76,** (1996).
5. M.S. Unlu *et al.*, J. Appl. Phys. **78,** R1-R33 (1995).

**QTuJ3** **3:00 pm**

## Modifications to blackbody radiation in a one-dimensional photonic bandgap structure

Jonathan P. Dowling, Mark J. Bloemer, Michael D. Tocci, Michael Scalora, Charles M. Bowden, *U.S. Army Aviation & Missile Command, AMSAM-RD-WS-ST, Redstone Arsenal, Alabama 35898-5000; E-mail: jdowling@ws.redstone.army.mil*

The Planck blackbody law is usually derived in a large cavity limit in which the density of electromagnetic modes is treated in the free-space continuum limit. However, in a one-dimensional (1D) photonic bandgap (PBG) material, the normal mode structure is manifestly different from in free space,[1-4] and hence the form of the blackbody spectrum can be radically altered. We calculate the modified blackbody frequency and wave-number spectrum in the simple example of 1D thin-film GaAs/AlGaAs PBG structure. Specifically, we compute the cavity-modified blackbody distribution as a function of frequency and wavevector and compare it to the experiment. (See Figs. 1 and 2.) As can be seen in the figures, the total power and the Lambertian angular distribution can be drastically modified depending on the location of the bulk blackbody spectral peak with respect to the photonic bandgap. In Sample A, Fig. 1, the spectral peak is aligned with the photonic band edge, leading to mission enhancement. In Sample B, Fig. 2, the blackbody peak is centered at the bandgap leading to suppression of emission. In both cases the angular distribution differs from the Lambertian expected for a bulk thermal emitter.

1. J.M. Bendickson, J.P. Dowling, M. Scalora, Phys. Rev. **53,** 4107 (1996).

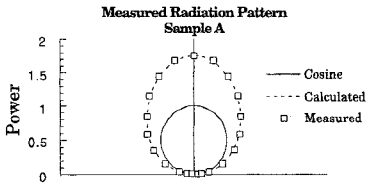


**QTuJ3 Fig. 1.** In Sample A, the spectral peak is aligned with the photonic band edge, leading to emission enhancement of the blackbody radiation and modification of the circular Lambertian emission profile.

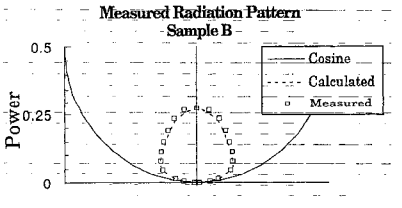


**QTuJ3 Fig. 2.** In Sample B, the spectral peak is aligned with the photonic bandgap, leading to emission suppression of the blackbody radiation and modification of the circular Lambertian emission profile.

2. J.P. Dowling and C.M. Bowden, Phys. Rev. A **46,** 612 (1992).
3. M. Scalora, J.P. Dowling, M.D. Tocci, M.J. Bloemer, C. Bowden, J.W. Haus, Appl. Opt. **60,** S57 (1995).
4. M.D. Tocci, M. Scalora, M.J. Bloemer, J.P. Dowling, C.M. Bowden, Phys. Rev. A **53,** 2799 (1996).

**QTuJ4** **3:15 pm**

## Reflection properties and defect formation in metallic photonic crystals

E. Özbay, B. Temelkuran, M. Sigalas,* G. Tuttle,* C.M. Soukoulis,* K.M. Ho,* *Department of Physics, Bilkent University, Bilkent Ankara 06533 Turkey*

Propagation of electromagnetic (EM) waves in periodic dielectric structures can be completely forbidden for a certain range of frequencies.[1] These three-dimensional arrays—photonic bandgap (PBG) crystals—can be used to engineer the properties of the radiation field within these structures. Although, the earlier work on photonic crystals concentrated on building structures using dielectric materials, there are certain advantages of introducing metals to photonic crystals.[2] First, the metals offer a higher rejection rate per layer when compared to dielectric crystals.[3] Second, for microwave applications the dimensions of metallic crystals can be kept much smaller than the minimum dimensions needed for a typical dielectric crystal.[4] In this paper, we investigate the reflection properties of layer-by-layer metallic photonic crystals, and use these properties to predict defect formation in layer-by-layer metallic photonic crystals.

In our investigations of reflection properties, we used metallic photonic crystals with the simple-tetragonal (st) structure. The reflection and transmission amplitude characteristics were measured by a network analyzer and standard gain horn antennas (Fig. 1). The properties of a 6-layer thick crystal along the stacking direction is shown in Fig. 2(a). Although the reflection-magnitude properties of the crystal were independent of the polarization vector e of the incident EM wave, we found a strong polarization dependence for the phase of the reflected waves. Figure 2(b) shows the phase of the reflected waves as a function of frequency for both polarizations. Figure 2(b) also shows the calculated

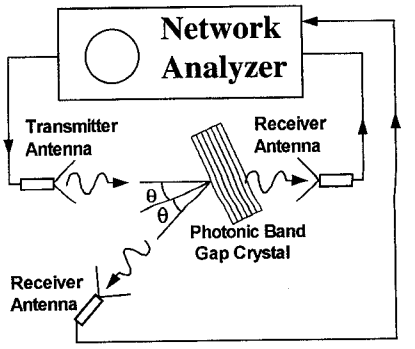


**QTuJ4 Fig. 1.** Experimental setup for measuring the reflection and transmission properties of the photonic crystals.

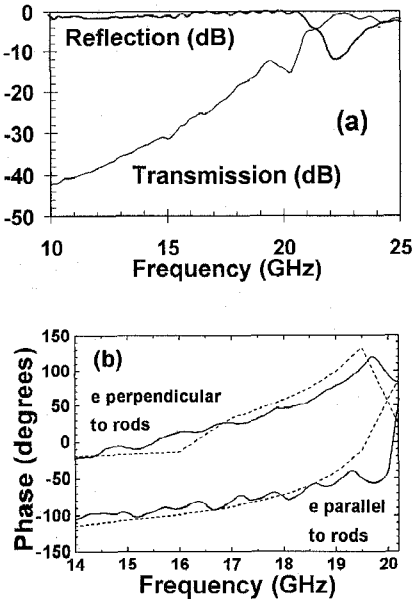


**QTuJ4 Fig. 2.** (a) Reflection (thick solid line) and transmission (thin solid line) characteristics of the photonic crystal. (b) Comparison of the theoretical (dashed) and experimental (solid) reflection-phase properties of the photonic crystal for different polarizations.

reflection-phase properties for the same structure, which was in good agreement with the experiment. We have used transfer matrix method (TMM) in our theoretical simulations.[5]

This phase information can also be interpreted as an effective distance (penetration depth) between the top surface and an ideal reflection plane inside the crystal. To account for the phase delay due to the reflection-phase, the EM waves can be considered to propagate a certain distance in the crystal and then reflect back from an ideal metallic plane with a phase shift of 180°.

The penetration depth information obtained from the reflection-phase measurements can be used to understand defect formation in Fabry–Perot type defect structures. A planar defect structure made of two photonic mirrors separated by a distance will have an effective cavity length. The length is equal to the sum of the penetration depths and the separation distance. This analogy then can be used to obtain penetration depths from the experimental defect frequencies. The values obtained from the defect frequency measurements (of cavities with different separation lengths) and the reflection phase measurements are compared in Fig. 3. As can be seen from the plot, there is a good agreement between the predicted and experimental penetration depths. The photonic mirrors have a typical penetration depth around 5 mm within the band gap frequencies. This information can be readily used to design a defect structure at a specified frequency.

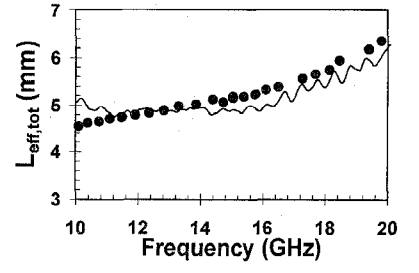


**QTuJ4 Fig. 3.** Comparison of the experimental (circles) and predicted effective reflection plane distances (solid line) of the Fabry–Perot cavity.

*Ames Laboratory and Microelectronics Research Center, Iowa State University, Ames, Iowa 50011*

1. K.M. Ho *et al.*, Phys. Rev. Lett. **65,** 3152 (1990).
2. D.F. Sievenpiper *et al.*, Phys. Rev. Lett. **76,** 2480 (1996).
3. E. Ozbay *et al.*, Appl. Phys. Lett. **69,** 3797 (1996).
4. J.S. McCalmont *et al.*, Appl. Phys. Lett. **68,** 2759 (1996).
5. M. Sigalas *et al.*, Phys. Rev. B **52,** 11744 (1995).

**QTuJ5 (Invited)** **3:30 pm**

## Experimental observation of interaction between Bragg solitons

B.J. Eggleton, R.E. Slusher,
N.M. Litchinitser,* G.P. Agrawal,*
A. Aceves,** C.M. de Sterke,† *Bell Laboratories, Lucent Technologies, Murray Hill, New Jersey 07974*

Possibly the most appealing property of optical solitons is their particlelike behavior. Solitons tend to survive perturbations and collisions and interact nondestructively with each other. Indeed for optical solitons which obey the integrable nonlinear Schrödinger equation the interaction can be either attractive or repulsive, depending on the relative phase of the two solitons.[1] In both cases the dynamics is well understood; either a periodic evolution (in the attractive case) or for the repulsive case a two soliton solution which is well approximated by the sum of two separated one soliton solutions. Bragg solitons,[2] on the other hand, are described by nonintegrable equations.[2–4] This means that, while they are also robust, in that they posses a particlelike behavior, they show the distinct signature of nonintegrability in that collisions are typically inelastic.[4] In this paper we report on experimental studies of interactions of Bragg solitons in optical fibers.

We investigated Bragg soliton interactions experimentally using the experimental setup shown in Fig. 1. We used a mode-locked Q-switched YLF laser, which generated 80-ps pulses at a repetition are of 500 Hz, having peak powers in excess of 10 kW. The pulses were first passed through a Mach–Zehnder interferometer to turn them into a pair of copolarized pulses. A precision translation stage (resolution 0.1 μm) in one arm of the interferometer allowed adjustment of the length of the arm allowing the pulse separation and relative phase to be varied. The detuning of the pulses from the Bragg resonance was chosen such that the length of the grating (6 cm), corresponded to five soliton periods, allowing ample opportunity for soliton interaction. At low powers the pulses were dispersed and no interaction was observed. The input power was then increased to 10 GW/cm$^2$, where the width of each pulse by itself reached a minimum value of 30 ps (deconvolved) at the output. Figure 2 shows a sample of our experimental results. In Fig. 2(a) the output is shown if the two arms of the interferometer are separately blocked in succession; it shows that initial separation between the pulses is approximately 50 ps. When the output from both arms is coupled into the fiber grating, the solitons interact. The separation of the output solitons is observed to depend on the relative phase between the two input pulses. Figure 2(b) shows the output intensity when the initial pulses are in phase, indicating the collapse of the two Bragg solitons. Figure 2(c), on the other hand, shows the output intensity when the initial pulses are out of phase, indicating a repulsive force. The dependence of the output pulse separation on the initial relative phase difference is indicative of the particlelike behavior of Bragg solitons.

Numerical simulations of the nonlinear coupled mode equations reveal that in spite of

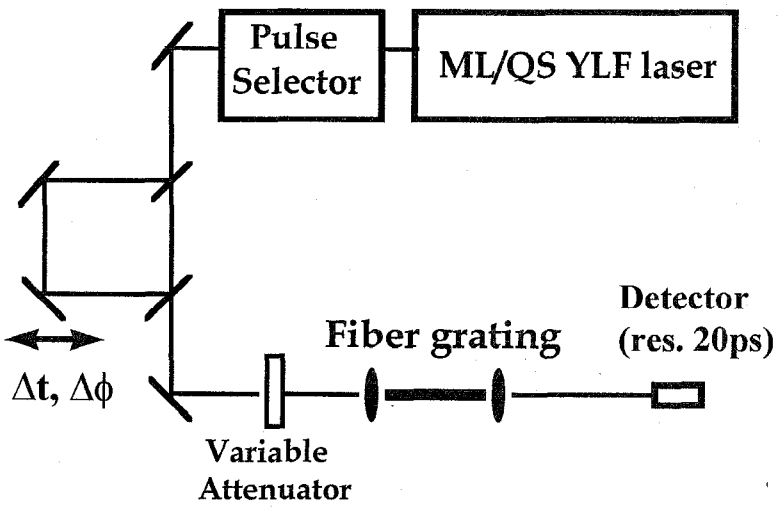


**QTuJ5 Fig. 1.** Experimental setup for launching two interacting Bragg solitons.